

Collective effects in multiparticle production processes at the LHC

S. M. Troshin, N. E. Tyurin

*Institute for High Energy Physics,
Protvino, Moscow Region, 142281, Russia*

Abstract

We discuss various aspects of the multiparticle production processes at the LHC energy range with emphasis on the collective effects associated with appearance of the new scattering mode, which corresponds to the reflective scattering and its impact on multiparticle production processes.

Introduction

Nowadays the LHC is collecting data and providing experimental results at the largest world energy $\sqrt{s} = 7 \text{ TeV}$. Along with realization of its discovery potential, the LHC experimental program renewed interest to the well known unsolved problems providing deepened insights into those issues. In this context the multiparticle production studies bring us a clue to the mechanisms of confinement and hadronization. Confinement of a color (i.e. the fact that an isolated color object has an infinite energy in the physical vacuum) is associated with collective, coherent interactions of quarks and gluons, and results in formation of the asymptotic states, which are the colorless, experimentally observable particles. The inelastic processes involve large number of particles in the final state. On the other side, the experimental measurements often reveal high degrees of a coherence in the relevant observables. No doubt these collective effects are very important for understanding of the nonperturbative collision dynamics. Such collective effects are associated, in particular, with unitarity regulating the relative strength of elastic and inelastic processes and connecting the amplitudes of the various multiparticle production processes. Unitarity for the scattering matrix is formulated for the asymptotic colorless on-mass shell states. There is no universal, generally accepted method to implement full unitarity in high energy scattering. A related problem of the absorptive corrections and of their sign has a long history of discussion (cf. [1] and references therein). However, a choice of particular unitarization scheme is not just a matter of taste.

Long time ago the arguments based on analytical properties of the scattering amplitude were put forward [2] in favor of the rational form of unitarization. It was shown that this form reproduced correct analytical properties of the scattering amplitude in the complex energy plane much easier compared to the exponential form. This specific form of unitarization [3] can be related to the confinement of color in QCD [4].

Correct account for the unitarity is essential for the minimum bias multiparticle production processes, correlations, anisotropic flows and studies of phase transitions.

The important point is that the region of the LHC energies is the one where the new, reflective scattering mode [5] can be observed. Such a mode naturally appears when energy grows and the rational form of unitarization being exploited [6]. This mode can be revealed at the LHC directly measuring $\sigma_{el}(s)$ and $\sigma_{tot}(s)$ [7]. The reflective scattering is correlated with the self-damping of the inelastic channels and leads to the asymptotically dominating role of elastic scattering, i. e. $\sigma_{el}(s)/\sigma_{tot}(s) \rightarrow 1$ at $s \rightarrow \infty$ while the both cross-sections, $\sigma_{el}(s)$ and $\sigma_{tot}(s)$, tend to infinity in this limit.

Of course, the obvious questions appear on compatibility of the reflective scat-

tering mode with dynamics of the multiparticle production, in particular, with the growth of the mean multiplicity in hadronic collisions with energy. Many models and the experimental data suggest a power-like energy dependence of mean multiplicity¹.

In this review we discuss relation of the reflective scattering with confinement and hadronization, in particular, we consider the effects of the reflective scattering in the multiparticle production processes at the LHC energies and apply a rational (U -matrix) unitarization method [3] to consider correlations in the multiparticle dynamics. We perform model calculations of global characteristics in the multiparticle production processes such as mean multiplicity, average transverse momentum, two-particle correlations, elliptic flow and demonstrate its quantitative and qualitative agreement with the first data obtained at the LHC. It appeared that reflective scattering leads to the prominent effects in the global observables and particle correlations.

1 Rational form of unitarization and confinement of colored degrees of freedom

Unitarity or conservation of probability, which can be written in terms of the scattering matrix as

$$SS^+ = 1, \quad (1)$$

implies an existence of the two scattering modes at high energies - shadowing and reflection. Saturation of the unitarity condition for the scattering matrix in hadron collisions at small impact parameters b , takes place when scattering acquires reflective nature, i.e. $S(s, b)|_{b=0} \rightarrow -1$ at $s \rightarrow \infty$. Here $S(s, b)$ is the elastic scattering S -matrix in the impact parameter representation. Approach to the full absorption in head-on collisions — the limit $S(s, b)|_{b=0} \rightarrow 0$ at $s \rightarrow \infty$ — does not follow from unitarity itself and is merely a result of the assumed saturation of the black disk limit. On the other hand, the reflective scattering is a natural interpretation of the unitarity saturation based on the optical concepts in high energy hadron scattering. Such reflective scattering can be traced to the continuous increasing density of the scatterer with energy, i.e. when density goes beyond some critical value relevant for the black disk limit saturation, the scatterer starts to acquire a reflective ability. The concept itself is quite general, and results from the S -matrix unitarity saturation related to the necessity to provide the total cross section growth at $s \rightarrow \infty$. This picture predicts that the scattering amplitude at the LHC energies is beyond the black disk limit at small impact parameters. The

¹Discussions of power-like energy dependence of mean hadronic multiplicity and list of references to the older papers can be found in [9, 10, 11]

consequences for the total, elastic and inelastic cross-sections have been discussed in [7].

Unitarity for the elastic scattering amplitude $F(s, t)$ can be written in the form

$$\text{Im}F(s, t) = H_{el}(s, t) + H_{inel}(s, t), \quad (2)$$

where $H_{el,inel}(s, t)$ are the corresponding elastic and inelastic overlap functions introduced by Van Hove [8]. Physical meaning of each term in Eq. (2) is evident from the graphical representation in Fig. 1. The functions $H_{el,inel}(s, t)$ are related

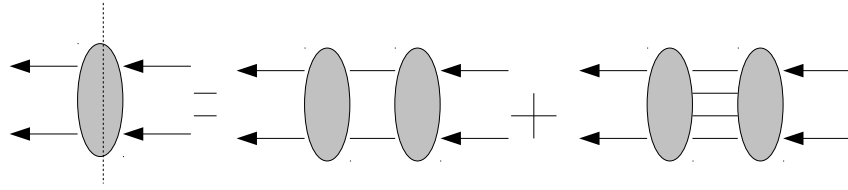


Figure 1: Eq. 2 in the graphical form.

to the functions $h_{el,inel}(s, b)$ via the Fourier-Bessel transforms, i.e.

$$H_{el,inel}(s, t) = \frac{s}{\pi^2} \int_0^\infty b db h_{el,inel}(s, b) J_0(b\sqrt{-t}). \quad (3)$$

The elastic and inelastic cross-sections can be obtained as follows:

$$\sigma_{el,inel}(s) \sim \frac{1}{s} H_{el,inel}(s, t = 0). \quad (4)$$

As it was already noted, the reflective scattering mode appears naturally in the U -matrix form of unitarization, where the $2 \rightarrow 2$ scattering matrix element in the impact parameter representation is the following linear fractional transform:

$$S(s, b) = \frac{1 + iU(s, b)}{1 - iU(s, b)}. \quad (5)$$

$U(s, b)$ is the generalized reaction matrix, which is considered to be an input dynamical quantity. The relation (5) is one-to-one transform and easily invertible.

Now, we would like to discuss relation of the rational unitarization form of scattering matrix with the confinement property of QCD. According to the confinement, isolated colored objects cannot exist in the physical vacuum and there is no room for objects like quark-proton scattering amplitude, since isolated color object has an infinite energy in the physical vacuum.

The important assumption in the derivation of the consequences of unitarity is the completeness of a set of the asymptotic states, those states include colorless

degrees of freedom or hadrons only. It can be considered as a questionable one in the QCD era. It might be reasonable to claim that a set of hadronic states does not provide a complete set of states and unitarity in the sense discussed above could be violated (cf. [12]). It was stated in this paper that the Hilbert space, which corresponds to colorless hadron states and is constructed using vectors spanned on the physical vacuum, should, in principle, be extended. At the present time it is often underlined that the vacuum state is not unique; i.e. the colored current quarks and gluons are in fact the degrees of freedom related to a different vacuum. Thus, the vacuum state may not be considered anymore to be the state of the lowest energy (ground state).

At the moment we would like to demonstrate that inclusion of the states corresponding to the confined objects (e.g. colored current or constituent quarks) into a set of the asymptotic states would lead to a rational form of S-matrix unitarization provided those states satisfy a certain constraint treated as a condition for confinement. We propose to manage these states similar to consideration of the states with indefinite metric in quantum electrodynamics as it was performed by N.N. Bogolyubov [13]. To construct the S matrix (which operates in the physical subspace) let us consider state vectors $|\Phi_{-}\rangle$ at $t \rightarrow -\infty$ and $|\Phi_{+}\rangle$ at $t \rightarrow +\infty$ each being the sum of the two vectors

$$|\Phi_{+}\rangle = |\varphi_{+}\rangle + |\omega_{+}\rangle$$

$$|\Phi_{-}\rangle = |\varphi_{-}\rangle + |\omega_{-}\rangle$$

where $|\varphi_{\pm}\rangle$ corresponds to the physical states and $|\omega_{\pm}\rangle$ – to the confined states. So, we have that $|\varphi_{\pm}\rangle = \mathcal{P}_{\pm}|\Phi_{\pm}\rangle$ and $|\omega_{\pm}\rangle = (1 - \mathcal{P}_{\pm})|\Phi_{\pm}\rangle$, where \mathcal{P}_{\pm} are the relevant projection operators relevant for the initial and final states, respectively.

The scattering operator $\tilde{\mathcal{S}}$ (defined as $|\Phi_{+}\rangle = \tilde{\mathcal{S}}|\Phi_{-}\rangle$) should not, in principle, conserve probability and obey unitarity condition since it operates in the Hilbert space which includes subspace where confined objects with an undefined norm reside. Next, let us to impose condition on the asymptotic vectors $|\omega_{\pm}\rangle$:

$$|\omega_{-}\rangle + |\omega_{+}\rangle = 0.$$

It means that *in*- and *out*- vectors corresponding to the states of the confined objects are just the mirror reflections of each other. Those reflections can be associated with the impossibility for confined objects to propagate outside the hadron. In quantum mechanics such solution corresponds to standing or stationary wave where on average net propagation of energy is absent. Thus, the rational form of unitary scattering operator \mathcal{S}

$$\mathcal{S} = \mathcal{P}_{+}\tilde{\mathcal{S}}[1 + (1 - \mathcal{P}_{+}\tilde{\mathcal{S}})]^{-1} \equiv (1 - \mathcal{U})(1 + \mathcal{U})^{-1},$$

in the physical subspace, i.e. $|\varphi_+\rangle = \mathcal{S}|\varphi_-\rangle$) can easily be obtained, since

$$|\varphi_+\rangle = \mathcal{P}_+ \tilde{\mathcal{S}}(|\varphi_+\rangle + |\omega_-\rangle).$$

We have started with scattering operator $\tilde{\mathcal{S}}$ in the Hilbert space which includes physical and unphysical subspaces and arrived to an unitary scattering operator \mathcal{S} in the physical subspace. Crucial assumption was a constraint for the states of confined objects from the unphysical subspace $|\omega_-\rangle + |\omega_+\rangle = 0$, which we assume to be related to the confinement condition. The imposition of this constraint is an equivalent to the statement that the scattering matrix in the unphysical subspace is identical with $-\mathbf{1}$. Thus, one can say that if scattering matrix in the space spanned over confined states is identically equal to $-\mathbf{1}$, then scattering matrix in the physical space is unitary. It is plausible therefore to assume that unitarity can be straightforwardly connected to confinement.

Rational or U -matrix form of unitarization was proposed long time ago [14] in the theory of radiation dumping. Self-damping of inelastic channels was considered in [15] and for the relativistic case such form of unitarization was obtained in [3]. It was demonstrated that it can be used for construction of a bridge between the physical states of hadrons and the states of the confined colored objects.

2 Reflective scattering at the LHC energies

In the rational form of unitarization the inelastic overlap function $h_{inel}(s, b)$ is connected with the function $U(s, b)$ by the relation

$$h_{inel}(s, b) = \frac{\text{Im}U(s, b)}{|1 - iU(s, b)|^2}, \quad (6)$$

and the only condition to obey unitarity is $\text{Im}U(s, b) \geq 0$. The elastic overlap function is related to the function $U(s, b)$ as follows

$$h_{el}(s, b) = \frac{|U(s, b)|^2}{|1 - iU(s, b)|^2}. \quad (7)$$

The form of $U(s, b)$ depends on particular model assumptions, but for qualitative purposes it is sufficient that it increases with energy in a power-like way and decreases with the impact parameter like a linear exponent or Gaussian. To simplify the qualitative picture, we consider also the function $U(s, b)$ as a pure imaginary. At sufficiently high energies ($s > s_R$), the two separate regions of impact parameter distances can be anticipated, namely the outer region of peripheral collisions where the scattering has a typical absorptive origin, i.e. $S(s, b)|_{b > R(s)} > 0$ and the

inner region of central collisions where the scattering has a combined reflective and absorptive origin, $S(s, b)|_{b < R(s)} < 0$.

We discuss now the impact parameter profiles of elastic and inelastic overlap functions for the scattering picture with reflection. The well known absorptive picture of high energy scattering corresponds to the black disk limit at $s \rightarrow \infty$. This limit has already been reached in the head-on proton–antiproton collisions at Tevatron, i.e. $h_{el}(s, b = 0) \simeq 0.25$ [16]. Thus, one can expect that in the framework of absorptive picture, black disk limit will be reached also at $b \neq 0$ at higher energies and the profiles of $h_{el}(s, b)$ and $h_{inel}(s, b)$ are to be similar and have a form close to step function (Fig. 2). We consider now energy evolution

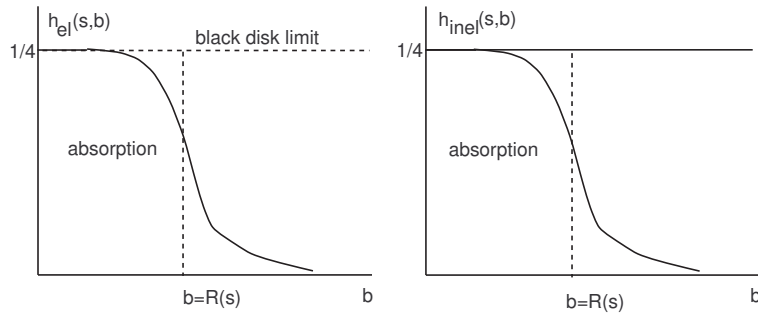


Figure 2: Typical picture of impact parameter profiles of the elastic and inelastic overlap function in the absorptive approach at asymptotic energies.

of the elastic and inelastic overlap functions which includes reflective scattering. With conventional parametrization of the U -matrix the inelastic overlap function increases with energies at modest values of s . It reaches its maximum value $h_{inel}(s, b = 0) = 1/4$ at some energy $s = s_R$ and beyond this energy the reflective scattering mode appears at small values of b . The region of energies and impact parameters corresponding to the reflective scattering mode is determined by the conditions $h_{el}(s, b) > 1/4$ and $h_{inel}(s, b) < 1/4$. The unitarity limit and black disk limit are the same for the inelastic overlap function, but these limits are different for the elastic overlap function. The quantitative analysis of the experimental data [17] gives the threshold value: $\sqrt{s_R} \simeq 2$ TeV. The function $h_{inel}(s, b)$ becomes peripheral when energy increases in the region $s > s_R$. At such energies the inelastic overlap function reaches its maximum at $b = R(s)$ where $R(s) \sim \ln s$. So, in the energy region, which lies beyond the transition threshold, there are two regions in impact parameter space: the central region of reflective scattering combined with absorptive scattering at $b < R(s)$ and the peripheral region of pure absorptive scattering at $b > R(s)$. Typical pattern of the impact parameter profiles for elastic

and inelastic overlap functions in the scattering picture with reflection at the LHC energies is depicted on Fig. 3.

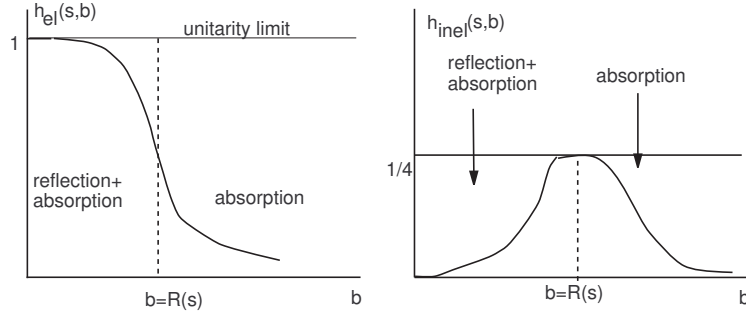


Figure 3: Typical qualitative picture of impact parameter profiles of the elastic and inelastic overlap function in the reflective approach at the asymptotically high energies.

It should be noted that at the values of energy $s > s_R$ the equation $U(s, b) = 1$ has a solution in the physical region of impact parameter values, i.e. $S(s, b) = 0$ at $b = R(s)$. This line is shown in the s and b plane in Fig. 4 alongside with the regions where elastic S -matrix has positive and negative values. The dependence

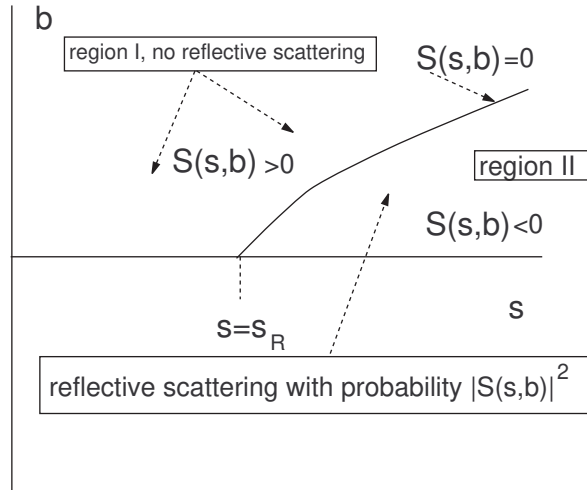


Figure 4: Regions of positive (absorptive scattering) and negative (absorptive and reflective scattering) values of the function $S(s, b)$ in the s and b plane.

of $S(s, b)$ on impact parameter b at fixed energies (in the region $s > s_R$) is depicted on Fig. 5.

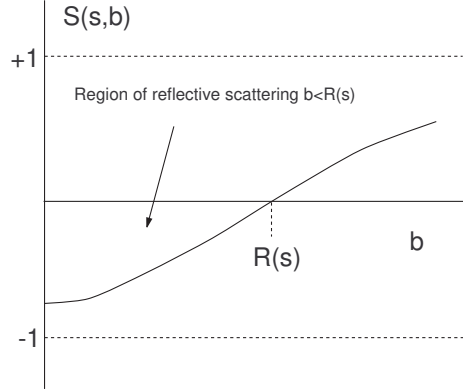


Figure 5: *Qualitative impact parameter dependence of the function $S(s, b)$ for the energies $s > s_R$.*

The probability of reflective scattering at $b < R(s)$ and $s > s_R$ is determined by the magnitude of $|S(s, b)|^2$; this probability is equal to zero at $s \leq s_R$ and $b \geq R(s)$ (region I on Fig.4). The behavior of $R(s)$ is determined by the logarithmic dependence $R(s) \sim \frac{1}{M} \ln s$. It is consistent with the analytical properties of the resulting elastics scattering amplitude in the complex t -plane and mass M can be related to the pion mass.

Thus, at the energies $s > s_R$ the reflective scattering will mimic presence of repulsive core in hadron and meson interactions as well. The generic geometrical picture at fixed energy beyond the black disc limit is described as a scattering off the partially reflective and partially absorptive disk surrounded by the black ring which becomes gray at larger values of the impact parameter. The evolution with energy is characterized by increasing albedo due to the interrelated increase of reflection and decrease of absorption at small impact parameters. Asymptotically, picture of particle collisions with small impact parameters looks like collisions of hard spheres.

3 Multiparticle production in the U -matrix approach

To consider multiparticle production in the U -matrix approach it should be noted first that

$$\text{Im}U(s, b) = \sum_{n \geq 3} \bar{U}_n(s, b), \quad (8)$$

where $\bar{U}_n(s, b)$ is a Fourier–Bessel transform of the function

$$\bar{U}_n(s, t) = \frac{1}{n!} \int \prod_{i=1}^n \frac{d^3 q_i}{q_{i0}} \delta^{(4)}\left(\sum_{i=1}^n q_i - p_a - p_b\right) U_n^*(q_1, \dots, q_n; p'_a, p'_b) \cdot U_n(q_1, \dots, q_n; p_a, p_b). \quad (9)$$

Here the functions $U_n(q_1, \dots, q_n; p_a, p_b)$ and $U_n(q_1, \dots, q_n; p_{a'}, p_{b'})$ correspond to the ununitarized (input or “Born”) amplitudes of the process

$$a + b \rightarrow 1 + \dots + n,$$

and the process with the same final state and the initial state with different momenta p'_a and p'_b

$$a' + b' \rightarrow 1 + \dots + n,$$

respectively. They are the analogs of the elastic U -matrix for the processes $2 \rightarrow n$. It is important to note that the functions $\bar{U}_n(s, t)$ are real ones (but not positively defined, contrary to the functions $\bar{U}_n(s, b)$). The impact parameter b is the variable which is conjugated to the variable $\sqrt{-t}$, where $t = (p_a - p'_a)^2$ and the following sum rule is valid for the function $I(s, b, q)$

$$\int \frac{d^3 q}{E} I(s, b, q) = \langle n \rangle (s, b) \text{Im} U(s, b). \quad (10)$$

The sum in the right hand side of the Eq. (9) runs over all inelastic final states $|n\rangle$ which include diffractive as well as non-diffractive ones. Graphically, these relations are illustrated in Fig. 6.

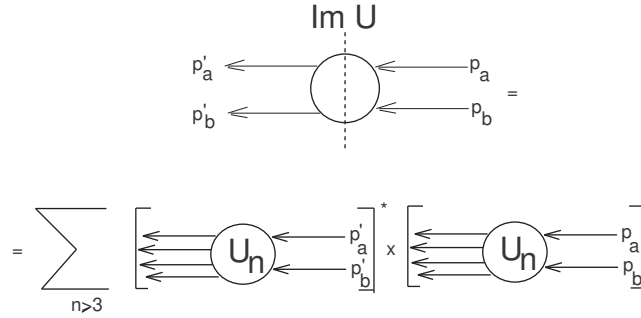


Figure 6: *Unitarity for the function ImU.*

Then the inclusive cross-section of the process $ab \rightarrow cX$ has the following form[18, 19], which is similar to the expression for the total inelastic cross-section:

$$E \frac{d\sigma}{d^3 q} = 8\pi \int_0^\infty b db \frac{I(s, b, q)}{|1 - iU(s, b)|^2}, \quad (11)$$

where $I(s, b, q)$ is the Fourier-Bessel transform of the functions which are defined similar to Eq. (9) but with the fixed momentum q and energy E of the particle c in the final state (Fig. 7).

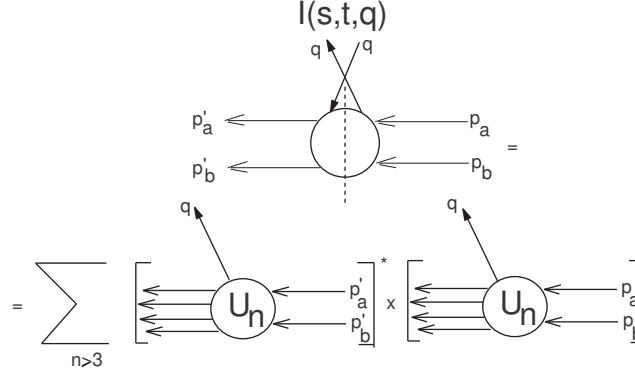


Figure 7: Unitarity for the function $I(s, t, q)$.

The impact parameter b is related to the impact parameters of the secondary particles by the relation [20]

$$\mathbf{b} = \sum_{i=1}^n x_i \mathbf{b}_i, \quad (12)$$

where x_i stands for the Feynman variable x of the i -th particle.

The general relations listed above reflect the unitarity saturation only and do not include other interaction dynamics. To provide further insight into the mechanism of multiparticle production additional assumptions on the quark-gluon hadron structure and their interaction dynamics should be adopted. It is described in the following two sections

4 Transient state of matter in hadron interactions

We assume that the transient states of matter in hadron and nuclei collisions have the same nature and originate from nonperturbative sector of QCD, associated with the mechanism of spontaneous chiral symmetry breaking (χ SB) in QCD [21]. Due to this mechanism transition of current into constituent quarks takes place, the latter ones are the quasiparticles whose masses are comparable with a typical hadron mass scale. These constituent quarks interact via exchange of the Goldstone bosons which are collective excitations of the condensate and are represented by pions (cf. e.g. [22]). The general form of the effective Lagrangian

($\mathcal{L}_{QCD} \rightarrow \mathcal{L}_{eff}$) relevant for description of the non-perturbative phase of QCD includes the three terms [23]

$$\mathcal{L}_{eff} = \mathcal{L}_\chi + \mathcal{L}_I + \mathcal{L}_C.$$

Here \mathcal{L}_χ is responsible for the spontaneous chiral symmetry breaking and turns on first. To account for the constituent quark interaction and their confinement the terms \mathcal{L}_I and \mathcal{L}_C are introduced. \mathcal{L}_I and \mathcal{L}_C do not affect the internal structure of the constituent quarks.

The picture of a hadrons consisting of the constituent quarks embedded into quark condensate implies that overlapping and interaction of the peripheral clouds occurs at the first stage of hadron interaction.

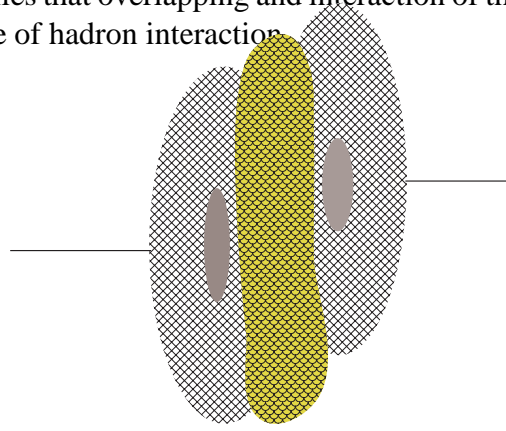


Figure 8: *Schematic view of initial stage of the hadron interaction.*

Nonlinear field couplings transform then some part of their kinetic energy into internal energy related to a mass [24, 25]. As a result we assume that the massive virtual quarks appear in the overlapping region and the effective field is generated in that way. This field is generated by QQ pairs and pions strongly interacting with quarks. In their turn pions themselves are bound states of the constituent quarks. At this stage the part of the effective Lagrangian \mathcal{L}_C is turned off (it turns on again in the final stage of the reaction) and interaction is described by \mathcal{L}_I . Its possible form was discussed in [26]. The transient phase (effective field) generation time Δt_{tp}

$$\Delta t_{tp} \ll \Delta t_{int},$$

where Δt_{int} is the total interaction time. This assumption on the almost instantaneous generation of the effective field has obtained a support in the very short thermalization time revealed in the heavy-ion collisions at RHIC [27, 28].

This picture assumes deconfinement at the initial stage of the hadron collisions and generation of the effective field common for both hadrons. Such ideas were used in the model [29] which has been applied to description of the elastic

scattering. Massive virtual quarks play a role of scatterers for the valence quarks in elastic scattering while their hadronization leads to production of the secondary particles. To estimate the number of such scatterers one could assume that certain part of hadron energy carried by the outer condensate clouds is being released in the overlap region to generate the massive quarks. Then this number can be estimated as

$$\tilde{N}(s, b) \propto \frac{(1 - \langle k_Q \rangle) \sqrt{s}}{m_Q} D_c^{h_1} \otimes D_c^{h_2} \equiv N_0(s) D_C(b), \quad (13)$$

where m_Q – constituent quark mass, $\langle k_Q \rangle$ – average fraction of hadron energy carried by the constituent valence quarks. Here the function D_c^h describes the condensate distribution inside the hadron h , and b is an impact parameter of the colliding hadrons. Thus, $\tilde{N}(s, b)$ massive quarks appear in addition to $N = n_{h_1} + n_{h_2}$ valence quarks. In elastic scattering those quarks are transient ones: they are transformed back into the condensates of the final hadrons. Calculation of the elastic scattering amplitude has been performed in [29]. However, valence quarks can excite a part of the cloud of the virtual massive quarks and those will subsequently fragment into the multiparticle final states. Such mechanism is responsible for the particle production and should lead to correlations between secondary particles which originate from the particular quark cluster resulting from the valence quark excitation. In this impact parameter picture the strong forward–backward multiplicity correlations should be expected.

Another mechanism contributing to the multiparticle production is a direct (i.e. not induced by interactions with valence quarks) hadronization of the massive quarks.

5 Multiparticle production mechanism

In sections 5 and 6 we consider correlations arising in the average multiplicity and transverse momentum behavior.

Remarkably, the existence of the massive quark-antiquark matter at the stage preceding hadronization seems to be supported by the experimental data obtained at CERN SPS and RHIC (see [30] and references therein).

Since the quarks are constituent, it is natural to expect direct proportionality between a secondary particles multiplicity and number of virtual massive quarks appeared in collision of the hadrons with given impact parameter:

$$\langle n \rangle(s, b) = \alpha(n_{h_1} + n_{h_2}) N_0(s) D_F(b) + \beta N_0(s) D_C(b), \quad (14)$$

with constant factors α and β and

$$D_F(b) \equiv D_Q \otimes D_C,$$

where the function $D_Q(b)$ is the probability amplitude of the interaction of valence quark, which is in fact related to the quark matter distribution in this hadron-like object [29]. The mean multiplicity $\langle n \rangle(s)$ can be calculated according to the formula

$$\langle n \rangle(s) = \frac{\int_0^\infty \langle n \rangle(s, b) h_{inel}(s, b) b db}{\int_0^\infty h_{inel}(s, b) b db}. \quad (15)$$

It is evident that the peripheral profile of $h_{inel}(s, b)$ associated with reflective scattering suppresses the region of small impact parameters and the main contribution to the mean multiplicity is due to the region of $b \sim R(s)$.

To make explicit calculations we model the condensate distribution $D_C(b)$ and the impact parameter dependence of the probability amplitude $D_Q(b)$ by the exponential forms with the different radii. Then the mean multiplicity

$$\langle n \rangle(s, b) = \tilde{\alpha} N_0(s) \exp(-b/R_F) + \tilde{\beta} N_0(s) \exp(-b/R_C). \quad (16)$$

The function $U(s, b)$ is chosen as a product of the averaged quark amplitudes

$$U(s, b) = \prod_{Q=1}^N \langle f_Q(s, b) \rangle. \quad (17)$$

This factorization originates from an assumption of a quasi-independent nature of the valence quark scattering, N is the total number of valence quarks in the colliding hadrons. The b -dependence of $\langle f_Q \rangle$ related to the quark formfactor $F_Q(q)$ has a simple form $\langle f_Q \rangle \propto \exp(-m_Q b/\xi)$. Thus, the generalized reaction matrix (in a pure imaginary case) gets the form [29]

$$U(s, b) = ig \left[1 + \alpha \frac{\sqrt{s}}{m_Q} \right]^N \exp(-Mb/\xi), \quad (18)$$

where $M = \sum_{q=1}^N m_Q$. At sufficiently high energies where increase of the total cross-sections is quite prominent we can neglect the energy independent term and rewrite the expression for $U(s, b)$ as

$$U(s, b) = ig \left(s/m_Q^2 \right)^{N/2} \exp(-Mb/\xi). \quad (19)$$

After calculation of the integrals (15) we arrive to the power-like dependence of the mean multiplicity $\langle n \rangle(s)$ at high energies

$$\langle n \rangle(s) = as^{\delta_F} + bs^{\delta_C}, \quad (20)$$

where

$$\delta_F = \frac{1}{2} \left(1 - \frac{\xi}{m_Q R_F} \right) \quad \text{and} \quad \delta_C = \frac{1}{2} \left(1 - \frac{\xi}{m_Q R_C} \right).$$

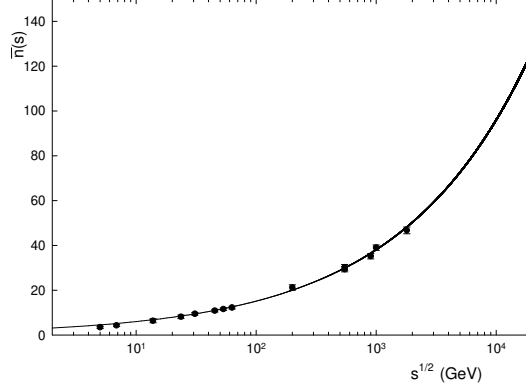


Figure 9: Energy dependence of mean multiplicity, theoretical curve is given by the equation $\langle n \rangle(s) = as^\delta$ ($a = 2.328$, $\delta = 0.201$).

There are four free model parameters, $\tilde{\alpha}$, $\tilde{\beta}$ and R_F , R_C , and the freedom in their choice is translated to a , b and δ_F , δ_C . The value of $\xi = 2$ is fixed from the data on angular distributions [29] and for the mass of constituent quark the standard value $m_Q = 0.35$ GeV was taken. However, fit to experimental data on the mean multiplicity leads to approximate equality $\delta_F \simeq \delta_C$ and actually Eq. (20) is reduced to the two-parametric power-like energy dependence of mean multiplicity

$$\langle n \rangle = as^\delta,$$

which is in good agreement with the experimental data (Fig. 9). Equality $\delta_F \simeq \delta_C$ means that variation of the correlation strength with energy is weaker than the power dependence and could be, e.g. a logarithmic one. From the comparison with the data on mean multiplicity we obtain that $\delta \simeq 0.2$, which corresponds to the effective masses, which are determined by the respective radii ($M = 1/R$), $M_C \simeq M_F \simeq 0.3m_Q$, i.e. $M_F \simeq M_C \simeq m_\pi$. The value of mean multiplicity expected at the LHC energy ($\sqrt{s} = 14$ TeV) is about 110.

Now we would like to make a remark on the mean multiplicity in the impact parameter representation. As it follows from the formulas of the section 2, the n -particle production cross-section $\sigma_n(s, b)$

$$\sigma_n(s, b) = \frac{\bar{U}_n(s, b)}{|1 - iU(s, b)|^2} \quad (21)$$

Then the probability

$$P_n(s, b) \equiv \frac{\sigma_n(s, b)}{\sigma_{inel}(s, b)} = \frac{\bar{U}_n(s, b)}{\text{Im}U(s, b)}. \quad (22)$$

Thus, we observe cancellation of the unitarity corrections in the ratio of the cross-sections $\sigma_n(s, b)$ and $\sigma_{inel}(s, b)$. Therefore the mean multiplicity in the impact parameter representation

$$\langle n \rangle(s, b) = \sum_n n P_n(s, b)$$

is not affected by unitarity corrections. However, the above cancellation of unitarity corrections does not take place for the quantity $\langle n \rangle(s)$. The main contribution to $\langle n \rangle(s)$ originates from peripheral values of the impact parameter. Thus, typical inelastic event at the LHC energies is the event with a nonzero value of the initial impact parameter of collision.

6 Rotation of transient matter and energy dependence of average transverse momentum

We are going now to evaluate energy dependence of the average transverse momentum of produced particles and propose a possible mechanism leading to this dependence. The geometrical picture of hadron collision discussed above implies that at high energies and non-zero impact parameters the constituent quarks produced in overlap region carry large orbital angular momentum. It can be estimated as

$$L(s, b) \propto b \frac{\sqrt{s}}{2} D_C(b). \quad (23)$$

Due to supposed strong interaction between the quarks this orbital angular momentum will lead to a coherent rotation of the quark system located in the overlap region as a whole. This rotation is similar to rotation of the liquid where strong correlations between particles momenta exist [31]. In what follows we argue that this collective coherent rotation would lead to the energy dependence of the average transverse momentum and can explain experimentally observed rising behavior of this quantity. It should be noted that discovery of the deconfined state of matter has been announced by four major experiments at RHIC [32]. Despite the highest values of energy and density have been reached, a genuine quark-gluon plasma QGP (gas of the free current quarks and gluons) was not observed. The deconfined state reveals the properties of the perfect liquid, being a strongly interacting collective state and therefore it was labeled as sQGP. Using similarity between the hadronic and nuclear interactions we assumed that transient state in hadron interactions is also a liquid-like strongly interacting matter. As it was already mentioned, the presence of large angular momentum in the overlap region will lead to coherent rotation of quark-pion liquid. Of course, there should be

experimental observations of this collective effect and one of them is the directed flow in hadron reactions, with fixed impact parameter discussed in [31]. It is not impossible task to measure impact parameter of collision in hadron reactions with the help of the event multiplicity studies. But effects averaged over impact parameter can be measured more easily using standard experimental techniques. So, it is natural to assume that the rotation of transient matter will affect average transverse momentum of the secondary hadrons in proton-proton collisions. Let for beginning do not take into account the other sources of the transverse momentum and temporally suppose that all average transverse momentum is a result of a coherent rotation of transient liquid-like state. Then the following relation can be invoked

$$\langle p_T \rangle(s, b) = \kappa L(s, b), \quad (24)$$

where $L(s, b)$ is given by Eq. (23) and κ is a constant which has dimension of inverse length. It is natural to relate it with inverse hadron radius, $\kappa \sim 1/R_h$. To calculate the average transverse momentum $\langle p_T(s) \rangle$ the following relation with $\langle p_T \rangle(s, b)$ will be used:

$$\langle p_T \rangle(s) = \frac{\int_0^\infty b db \langle p_T \rangle(s, b) \langle n \rangle(s, b) h_{inel}(s, b)}{\int_0^\infty b db \langle n \rangle(s, b) h_{inel}(s, b)} \quad (25)$$

where $h_{inel}(s, b)$ is the inelastic overlap function. Now calculating the respective integrals we obtain the power-like dependence of the average transverse momentum $\langle p_T \rangle(s)$ at high energies

$$\langle p_T \rangle(s) = c s^{\delta_C}, \quad (26)$$

where

$$\delta_C = \frac{1}{2} \left(1 - \frac{\xi}{m_Q R_C} \right).$$

The value of ξ is obtained from the data on angular distributions [29] and for the mass of constituent quark the standard value $m_Q = 0.35$ GeV is taken. Of course, besides collective effects average transverse momentum would get contributions from other sources such as thermal distribution proposed long time ago by Hagedorn [33]. This part has no energy dependence and we take it into account by simple addition of the constant term to the power-dependent one, i.e.:

$$\langle p_T \rangle(s) = a + c s^{\delta_C} \quad (27)$$

Existing experimental data can be described well (cf. Fig. 10) using Eq. (27) with parameters $a = 0.337$ GeV/c, $c = 6.52 \cdot 10^{-3}$ GeV/c and $\delta_C = 0.207$. The numerical value of R_C is determined by pion mass with better than 10%

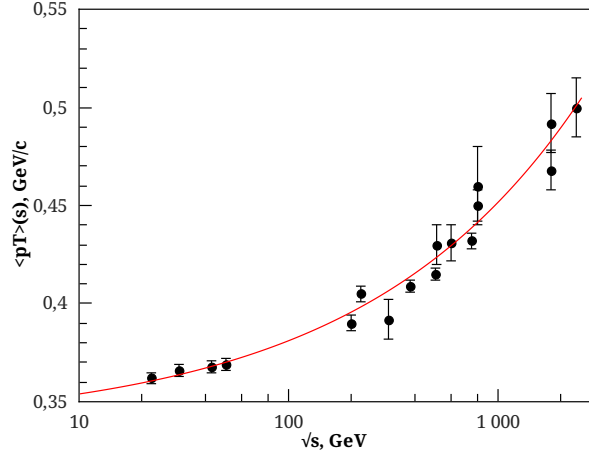


Figure 10: *Energy dependence of the average transverse momentum in pp-collisions, experimental data from [34, 35].*

precision, $R_C \simeq 1/m_\pi$. In the model the indices in the energy dependencies of average multiplicity and transverse momentum δ and δ_C are determined by the same expression and experimental data fitting with free parameters δ and δ_C confirms this coincidence with better than 10% precision also; note that the value $\delta = 0.201$ follows from the experimental data analysis for the average multiplicity.

7 Elliptic flow in proton collisions at the LHC energies

As it was already noted the most typical inelastic event at the LHC energies occurs with nonzero impact parameter. We consider therefore in this section peripheral hadronic collisions. The orientation of the reaction plane in pp -collisions can therefore be determined.

There are several experimental probes of collective dynamics. Some of them were considered in the previous sections. Another observables are related to the anisotropic flows and among them the most widely discussed one is the elliptic flows

$$v_2(p_T) \equiv \langle \cos(2\phi) \rangle_{p_T} = \left\langle \frac{p_x^2 - p_y^2}{p_T^2} \right\rangle, \quad (28)$$

which is the second Fourier moment of the azimuthal momentum distribution of the particles with a fixed value of p_T . The azimuthal angle ϕ is an angle of the detected particle with respect to the reaction plane, which is spanned by the colli-

sion axis z and the impact parameter vector \mathbf{b} . The impact parameter vector \mathbf{b} is directed along the x axis. Averaging is taken over a large number of the events. Elliptic flow can be expressed in covariant form in terms of the impact parameter and transverse momentum correlations as follows

$$v_2(p_T) = \left\langle \frac{(\hat{\mathbf{b}} \cdot \mathbf{p}_T)^2}{p_T^2} \right\rangle - \left\langle \frac{(\hat{\mathbf{b}} \times \mathbf{p}_T)^2}{p_T^2} \right\rangle, \quad (29)$$

where $\hat{\mathbf{b}} \equiv \mathbf{b}/b$. To get some hints on the possible behavior of the elliptic flow in proton collisions, it is useful to recollect what is known on this observable from nuclear collisions experiments. Integrated elliptic flow v_2 at high energies is positive and increases with $\sqrt{s_{NN}}$. The differential elliptic flow $v_2(p_T)$ increases with p_T at small values of transverse momenta, then it becomes flatten in the region of the intermediate transverse momenta and decreases at large p_T . It is also useful to apply a simple geometrical ideas which imply existence of the elliptic flow in hadronic reactions. Geometrical notions for description of multiparticle production in hadronic reactions were used by many authors, e.g by Chou and Yang in [36]. In the peripheral hadronic collisions the overlap region has different sizes along the x and y directions. According to the uncertainty principle we can estimate the value of p_x as $1/\Delta x$ and correspondingly $p_y \sim 1/\Delta y$ where Δx and Δy characterize the size of the region where the particle originate from. Taking $\Delta x \sim R_x$ and $\Delta y \sim R_y$, where R_x and R_y characterize the sizes of the almond-like overlap region in transverse plane, we can easily obtain proportionality of v_2 in collisions with fixed initial impact parameter to the eccentricity of the overlap region, i.e.

$$v_2 \sim \frac{R_y^2 - R_x^2}{R_x^2 + R_y^2}. \quad (30)$$

The presence of correlations of impact parameter vector \mathbf{b} and \mathbf{p}_T in hadron interactions follows also from the relation between impact parameters in the multiparticle production:

$$\mathbf{b} = \sum_i x_i \mathbf{b}_i. \quad (31)$$

Here x_i stand for Feynman x_F of i -th particle, the impact parameters \mathbf{b}_i are conjugated to the transverse momenta $\mathbf{p}_{i,T}$.

The above considerations are based on the uncertainty principle and angular momentum conservation, but they do not preclude the existence of the dynamical description, which will be discussed in the next section

As it was noted in the section 6 an essential point of the proposed production mechanism is the rotation of the transient state due to the presence of a non-zero impact parameter in the collision. The unitarity saturation invokes a dynamical

mechanism leading to the peripheral nature of inelastic collisions at the LHC energies. One can suggest therefore that the events with average and higher multiplicity at the LHC energy $\sqrt{s} = 7$ TeV correspond to the peripheral hadron collisions. Of course, the standard inclusive cross-section for unpolarized particles being integrated over impact parameter \mathbf{b} , does not depend on the azimuthal angle of the detected particle transverse momentum.

When the impact parameter vector \mathbf{b} and transverse momentum \mathbf{p}_T of the detected particle are fixed the function I does depend on the azimuthal angle ϕ between vectors \mathbf{b} and \mathbf{p}_T . The dependence on the azimuthal angle ϕ can be written in explicit form through the Fourier series expansion

$$I(s, \mathbf{b}, y, \mathbf{p}_T) = \frac{1}{2\pi} I_0(s, b, y, p_T) \left[1 + \sum_{n=1}^{\infty} 2\bar{v}_n(s, b, y, p_T) \cos n\phi \right]. \quad (32)$$

The function $I_0(s, b, \xi)$ satisfies to the following sum rule

$$\int I_0(s, b, y, p_T) p_T dp_T dy = \langle n \rangle(s, b) \text{Im} U(s, b), \quad (33)$$

where $\langle n \rangle(s, b)$ is the mean multiplicity depending on impact parameter. Thus, the bare anisotropic flow $\bar{v}_n(s, b, y, p_T)$ is related to the measured flow v_n as follows

$$v_n(s, b, y, p_T) = w(s, b) \bar{v}_n(s, b, y, p_T).$$

where the function $w(s, b)$ is

$$w(s, b) \equiv |1 - iU(s, b)|^{-2}.$$

In the above formulas the variable y denotes rapidity, i.e. $y = \sinh^{-1}(p/m)$, where p is a longitudinal momentum. Thus, we can see that unitarity corrections are mostly important at small impact parameters, i.e. they modify anisotropic flows at small centralities, while peripheral collisions are almost not affected by unitarity.

Now we are going to use the particle production mechanism described above for evaluation of the elliptic flow in pp -interactions. It was suggested that the rotation of transient matter will affect the average transverse momentum of the secondary hadrons produced in proton-proton collisions. Going further, one should be more specific and note that, in fact, the rotation gives a contribution to the x -component of the transverse momentum and does not contribute to the y -component of the transverse momentum, i.e.

$$\Delta p_x = \kappa L(s, b) \quad (34)$$

while

$$\Delta p_y = 0. \quad (35)$$

Assuming that $p_x = p_0 + \Delta p_x$ ($\Delta p_x \ll p_0$) and $p_y = p_0$, the contribution into the elliptic flow of the transient matter rotation can be calculated by analogy with the average transverse momentum calculation performed in [37]. The resulting integral elliptic flow increases with energy

$$v_2 \propto s^{\delta_C},$$

where $\delta_C = 0.207$. It should be noted here that transient matter consists of virtual constituent quarks strongly interacting via pion (Goldstone bosons) exchanges.

The incoming constituent quark has a finite geometrical size determined by the radius r_Q and interaction radius R_Q ($R_Q > r_Q$). The former one is determined by the chiral symmetry breaking mechanism and the latter one — by the confinement radius. Meanwhile, it is natural to suppose on the base of the uncertainty principle that size of the region where the virtual massive quark Q is knocked out from the cloud is determined by its transverse momentum, i.e. $\bar{R} \simeq 1/p_T$. However, it is evident that \bar{R} cannot be larger than the interaction radius of the valence constituent quark R_Q . It is also clear that \bar{R} should not be less than the geometrical size of the valence constituent quark r_Q for this mechanism be a working one. When \bar{R} becomes less than r_Q , this constituent quark mechanism does not work anymore and one should expect vanishing collective effects in the relevant region of the transverse momentum.

The value of the quark interaction radius was obtained under analysis of the elastic scattering [29] and it has the following dependence on its mass

$$R_Q = \xi/m_Q \sim 1/m_\pi \quad (36)$$

where $\xi \simeq 2$ and therefore $R_Q \simeq 1 \text{ fm}$, while the geometrical radius of quark r_Q is about 0.2 fm . It should be noted the region, which is responsible for the small- p_T hadron production, has large transverse dimension and the incoming constituent quark excites the rotating cloud of quarks with different values and directions of their momenta in that case. Effect of rotation will therefore be smeared off over the volume $V_{\bar{R}}$ and then one should expect that $\langle \Delta p_x \rangle_{V_{\bar{R}}} \simeq 0$. Thus,

$$v_2^Q(p_T) \equiv \langle v_2 \rangle_{V_{\bar{R}}} \simeq 0 \quad (37)$$

at small p_T . When we proceed to the region of higher values of p_T , the radius \bar{R} is decreasing and the effect of rotation becomes more and more prominent, incoming valence quark excites now the region where most of the quarks move coherently, in the same direction, with approximately the same velocity. The mean value $\langle \Delta p_x \rangle_{V_{\bar{R}}} > 0$ and

$$v_2^Q(p_T) \equiv \langle v_2^Q \rangle_{V_{\bar{R}}} > 0 \quad (38)$$

and it increases with p_T . The increase of v_2^Q with p_T will disappear at $\bar{R} = r_Q$, i.e. at $p_T \geq 1/r_Q$, and saturation will take place. The value of transverse momentum where the flattening starts is about $1 \text{ GeV}/c$ for $r_Q \simeq 0.2 \text{ fm}$. At very large transverse momenta the constituent quark picture would not be valid and elliptic flow vanishes as it was already mentioned.

We discussed elliptic flow for the constituent quarks. Predictions for the elliptic flow for the hadrons depends on the supposed mechanism of hadronization. For the intermediate values of p_T the constituent quark coalescence mechanism [38, 39] would be dominating one. In that case the hadron elliptic flow can be obtained from the constituent quark one by the replacement $v_2 \rightarrow n_V v_2^Q$ and $p_T \rightarrow p_T^Q/n_V$, where n_V is the number of constituent quarks in the produced hadron.

Typical qualitative dependence of elliptic flow in pp -collisions in this approach is presented in Fig.11

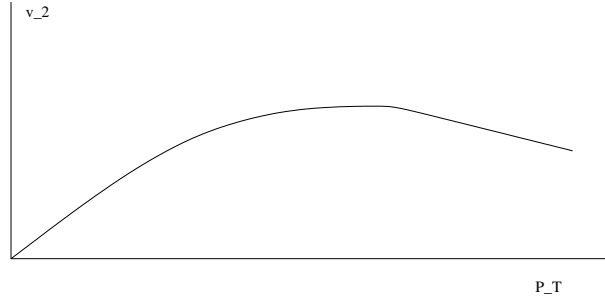


Figure 11: *Qualitative dependence of the elliptic flow v_2 on transverse momentum in pp -collisions.*

The centrality dependence of the elliptic flow is determined by the orbital angular momentum L dependence on the impact parameter, i.e. it should be decreasing towards high and low centralities. Decrease toward high centralities is evident since no overlap of hadrons should occur at high enough impact parameters. Decrease of v_2 toward lower centralities is specific prediction of the proposed mechanism based on rotation since the central collisions with smaller impact parameters would lead to slower rotation or its complete absence in the head-on collisions (it is also result of the symmetry in head-on collisions). Qualitative dependence of the elliptic flow on the impact parameter is similar to the one depicted in Fig.11 where variable b is to be used instead of transverse momentum.

8 Two-particle correlations in pp -collisions

The ridge structure was observed first at RHIC in the two-particle correlation function in the near-side jet production. It was demonstrated that the ridge particles have a narrow $\Delta\phi$ correlation distribution (where ϕ is an azimuthal angle) and wide $\Delta\eta$ correlations (η is a pseudorapidity). The ridge phenomenon was associated with the collective effects of a medium [40].

The similar structure in the two-particle correlation function was observed by the CMS Collaboration [41]. This is rather surprising result because the ridge structure was observed for the first time in pp -collisions. Those collisions are commonly treated as the “elementary” ones under the heavy-ion studies and therefore often used as the reference process for detecting deconfined phase formation on the base of difference between pp - and AA -collisions. It is evident now that such approach should be revised in view of this new and unexpected experimental result.

In the proposed explanation of the ridge effect at the LHC energy $\sqrt{s} = 7$ TeV a dynamical selection of peripheral region in impact parameter space responsible for the inelastic processes is the important point. As it was already noted, the geometrical picture of hadron collision at non-zero impact parameters implies that the generated massive virtual quarks in overlap region could obtain very large initial orbital angular momentum at high energies. Due to strong interaction between the quarks this orbital angular momentum leads to the coherent rotation of the quark system located in the overlap region as a whole in the xz -plane. This rotation is similar to the rotation of liquid. The assumed particle production mechanism at moderate transverse momenta is an excitation of a part of the rotating transient state of massive constituent quarks (interacting by pion exchanges). Due to the

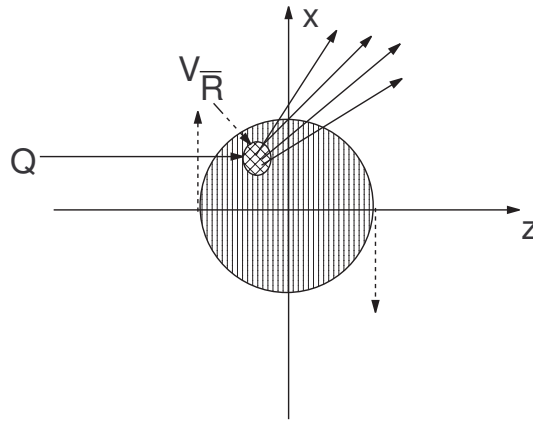


Figure 12: *Interaction of the constituent quark with rotating quark-pion liquid.*

fact that the transient matter is strongly interacting, the excited parts should be located closely to the periphery of the rotating transient state otherwise absorption would not allow quarks and pions leave the interaction region (quenching).

The mechanism is sensitive to the particular direction of rotation and to the rotation plane orientation. This will lead to the narrow distribution of the two-particle correlations in $\Delta\phi$. However, two-particle correlation could have broad distribution in polar angle ($\Delta\eta$) in the above mechanism (Fig. 12). Quarks in the excited part of the cloud could have different values of the two components of the momentum (with its third component lying in the rotation xz -plane) since the excited region V_R has significant extension.

Thus, the ridge-like structure observed in the high multiplicity events by the CMS Collaboration can be considered as experimental manifestation of the coherent rotation of the transient matter in hadron collisions. The narrow two-particle correlation distribution in the azimuthal angle is the distinctive feature of this mechanism.

There should be other experimental observations of this collective effect. One was mentioned already. It is the directed flow v_1 in hadron reactions, with fixed impact parameter discussed in [31]. Rotation of transient matter will affect also elliptic flow v_2 and average transverse momentum of the secondary particles produced in proton-proton collisions.

The ridge effect has triggered flow of possible explanation using different mechanisms [42, 43, 44, 45, 46, 47, 48, 49, 50, 51, 52].

The one described in this paper and in [53] relates appearance of the ridge effect with the reflective scattering at the LHC energies. Absence of the reflective scattering at lower energies explains why the ridge effect was not observed at the ISR or Tevatron. This important point on the ridge energy dependence needs to be explained by any particular mechanism proposed as a source of the two-particle correlations.

9 Genuine QGP formation

The dynamical mechanism of the average transverse momentum growth, anisotropic flows v_1 , v_2 , two-particle correlations (ridge) originate from the collective effect of transient matter rotation, while dynamics of average multiplicity growth is related to the mechanism where a nonlinear field couplings transform the kinetic energy to internal energy. Formation of a genuine quark-gluon plasma in transient state in the form of the noninteracting gas of free quarks and gluons would result in disappearance of the effects of rotation of the transient state. Vanishing the energy dependent contribution to the average transverse momentum should therefore be expected, i.e. average transverse momentum would reach maximum at some

energy and then will decrease till eventual flat behavior (cf. Fig.13). Vanishing

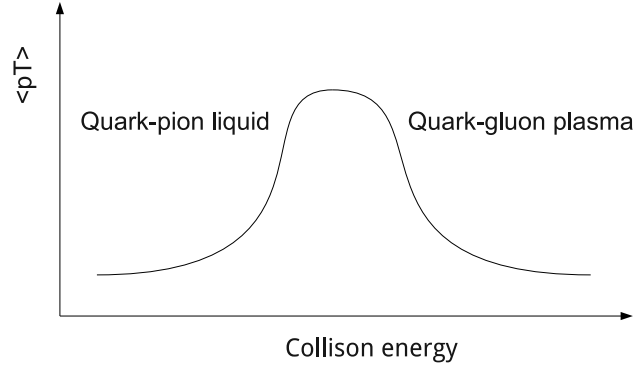


Figure 13: *Qualitative energy dependence of the average transverse momentum in pp-collisions in case of genuine QGP formation at super high energies.*

rotation will lead to vanishing anisotropic flows v_1 and v_2 . Of course, this picture is a rather qualitative one since the nature of phase transition from strongly interacting matter (associated with quark-pion liquid in the model) to the genuine quark-gluon plasma is not known. Currently, there is no experimental indications that such a transition will indeed take place at super high energies. At the same time there are theoretical arguments that existence of genuine QGP (ideal gas) would contradict to the confinement property of QCD. This contradiction arises in the many dynamical mechanisms of hadronization [54, 55]. However, the issue of the genuine QGP existence can only be resolved by the experimental searches.

It should be noted that inverse phase transition (from parton gas in parton model to liquid) could explain a saturation phenomena in deep inelastic processes [56].

The natural question appears about the role of orbital angular momentum in those mentioned above phase transitions.

10 Spin correlations due to reflective scattering in the case of genuine QGP formation

It is interesting to make a conclusion on the possible effect of the imbalance of the orbital angular momentum in the case of the genuine QGP formation. It should be noted that we can consider separately particles production in the forward and backward hemispheres [57]. Let us consider for example particles produced in

the forward hemisphere. The orbital angular momentum in the initial state can be estimated as

$$L_i \simeq \frac{\sqrt{s}}{2} \frac{R(s)}{2}, \quad (39)$$

where $R(s)$ is the interaction radius. The orbital angular momentum in the final state is then

$$L_f \simeq \frac{\langle n \rangle(s) \langle x_L \rangle(s) \sqrt{s}}{4} \frac{R(s)}{2}, \quad (40)$$

where we have taken into account that $\langle n \rangle(s)/2$ particles with the average fraction of their longitudinal momentum $\langle x_L \rangle(s)$ are produced at the impact parameter $R(s)/2$ due to reflective scattering. The average fraction of longitudinal momentum $\langle x_L \rangle(s)$ according to the hypothesis of limiting fragmentation [58] would not decrease with energy. Thus we arrive to the negative imbalance of the orbital angular momentum

$$\Delta L = L_i - L_f \simeq \frac{\sqrt{s}}{2} \frac{R(s)}{2} \left(1 - \frac{\langle n \rangle(s) \langle x_L \rangle(s)}{2}\right), \quad (41)$$

i.e.

$$\Delta L \simeq -\frac{\sqrt{s}}{2} \frac{R(s)}{2} \frac{\langle n \rangle(s) \langle x_L \rangle(s)}{2}. \quad (42)$$

This negative ΔL should be compensated by the total positive spin S of final particles (since the particles in the initial state are unpolarized)

$$S = -\Delta L \quad (43)$$

This spin alignment of produced particles appears in the reflective scattering mode when the particles are produced in the region of impact parameters $b = R(s)$.

The vector of spin \vec{S} lies in the transverse plane but it cannot be detected through the transverse polarization of single particle due to azimuthal symmetry of the production process (integration over azimuthal angle φ). However, this effect can be traced measuring transverse spin correlations of two particles $\langle s_i s_j \rangle$. The most evident way to reveal this effect is to perform the measurements of the spin correlations of hyperons whose polarizations can be extracted from the angular distributions of their weak decay products.

Spin correlation should be stronger for the light particles and the weakening is expected for heavy particles since they should be produced at smaller values of impact parameters.

Thus, we can expect appearance at the LHC energies of strong spin correlations of final particles as a result of the prominent reflective scattering mode in the case if genuine QGP is formed in the transient state. Vanishing anisotropic flows, decreasing average transverse momentum and appearance (simultaneous) of the secondary particles polarization are thus the signals of the genuine QGP formation.

11 Effects of the reflective scattering mode for nuclear collisions

In this final section we proceed from proton collisions to the collisions of nuclei. Consider central collision of two identical nuclei having N nucleons in total with center of mass energy \sqrt{s} per nucleon and calculate nucleon density $n_R(T, \mu) = N/V$ in the initial state at given temperature T and baryochemical potential μ in the presence of the reflective scattering. The effect of the reflective scattering of hadrons is equivalent to decrease of the volume of the available space which the hadrons are able to occupy in the case when reflective scattering is absent. Thus followings to van der Waals method, we must then replace volume V by $V - p_R(s)V_R(s)\frac{N}{2}$, i.e. we should write

$$n(T, \mu) = \frac{N}{V - p_R(s)V_R(s)\frac{N}{2}},$$

where $n(T, \mu)$ is hadron density without account for reflective scattering and $p_R(s)$ is the averaged over volume $V_R(s)$ probability of reflective scattering:

$$p_R(s) = \frac{1}{V_R(s)} \int_{V_R(s)} |S(s, r)|^2 d^3x.$$

The volume $V_R(s)$ is determined by the radius of the reflective scattering. Here we assume spherical symmetry of hadron interactions, i.e. we replace impact parameter b by r and approximate the volume $V_R(s)$ by $V_R(s) \simeq (4\pi/3)R^3(s)$. Hence, the density $n_R(T, \mu)$ is connected with corresponding density in the approach without reflective scattering $n(T, \mu)$ by the following relation

$$n_R(T, \mu) = \frac{n(T, \mu)}{1 + \alpha(s)n(T, \mu)},$$

where $\alpha(s) = p_R(s)V_R(s)/2$. Let us now estimate change of the function $n_R(T, \mu)$ due to the presence of reflective scattering. We can approximate $p_R(s)$ by the value of $|S(s, b=0)|^2$ which tends to unity at $s \rightarrow \infty$. It should be noted that the value $\sqrt{s_R} \simeq 2 \text{ TeV}$ [17]. Below this energy there is no reflective scattering, $\alpha(s) = 0$ at $s \leq s_R$, and therefore corrections to the hadron density are absent. Those corrections are small when the energy is not too much higher than s_R . At $s \geq s_R$ the value of $\alpha(s)$ is positive, and presence of reflective scattering diminishes hadron density. We should expect that this effect would already be noticeable at the LHC energy $\sqrt{s} \simeq 5 \text{ TeV}$ in $Pb + Pb$ collisions. At very high energies ($s \rightarrow \infty$)

$$n_R(T, \mu) \sim 1/\alpha(s) \sim M^3 / \ln^3 s.$$

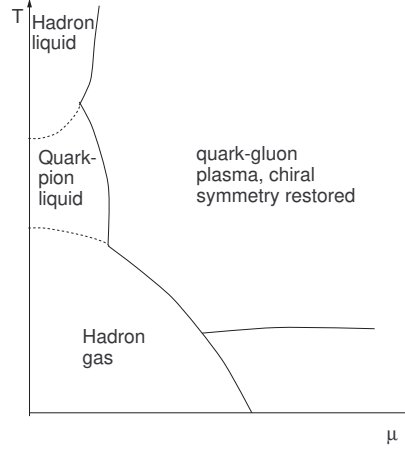


Figure 14: *Phases of strongly interacting matter.*

This limiting dependence for the hadron density appears due to the presence of the reflective scattering which results in similarity of head-on hadron collisions with scattering of hard spheres. It should be noted that this dependence has been obtained under assumption on spherical symmetry of hadron interaction region. Otherwise, limiting dependence of the hadron density in transverse plane can only be obtained, i.e. transverse plane density of hadrons would have then the following behavior

$$n_R(T, \mu) \sim M^2 / \ln^2 s.$$

Thus, the following chain of transitions between different (physical and non-perturbative) vacuum states can be foreseen as the temperature increases at the constant value of chemical potential μ :

$$|0\rangle_{ph}(\text{Hadron gas}) \rightarrow |0\rangle_{np}(\text{Quark-pion liquid}) \rightarrow |0\rangle_{ph}(\text{Hadron liquid}).$$

The corresponding phase diagram depicted in Fig. 14.

Thus, the reflective scattering mode can help in searches of the deconfined state and studies of transition mechanism to this state of matter.

Acknowledgement

We had pleasure discussing results described in this paper with N. Buttimore, J. Cudell, M. Islam, L. Jenkovszky, A. Krisch, E. Levin, I. Lokhtin, U. Maor, A. Martin, E. Martynov, V. Petrov, A. Prokudin, J. Ralston, V. Savrin, D. Sivers and O. Teryaev.

References

- [1] C. T. Sachrajda and R. Blankenbecler, Phys. Rev. D **12**, 1754 (1975).
- [2] R. Blankenbecler and M. L. Goldberger. Phys. Rev. **126**, 766 (1962) .
- [3] A. A. Logunov, V. I. Savrin, N. E. Tyurin and O. A. Khrustalev, Teor. Mat. Fiz. **6**, 157 (1971).
- [4] S.M. Troshin, N.E. Tyurin, Mod. Phys. Lett. A **25**, 3363 (2010).
- [5] S.M. Troshin, N.E. Tyurin, Int. J. Mod. Phys. A**22**, 4437 (2007).
- [6] S.M. Troshin, N.E. Tyurin, Phys. Lett. B**316**, 175 (1993).
- [7] S. M. Troshin and N. E. Tyurin, Eur. Phys. J. C **21**, 679 (2001).
- [8] L. Van Hove, Nuovo Cimento, **28**, 798 (1963).
- [9] A.M. Polyakov, Sov. Phys. JETP **32**, 296 (1971)
- [10] S. Barshay, P. Heiliger, Mod. Phys. Lett. A **7**, 1749 (1992).
- [11] P.C. Beggio, M.J. Menon and P. Valin. Phys. Rev. D **61**, 034015 (2000).
- [12] J.P. Ralston, *J. Phys. Conf. Ser.* **69**, 012030 (2007).
- [13] N.N. Bogolyubov, *Proceedings of 1958 Annual Conference on High Energy Physics at CERN*, p. 129, Ed. B. Ferretti, CERN, 1958.
- [14] W. Heitler, *Proc. Cambr. Phil. Soc.*, **37**, 291 (1941).
- [15] M. Baker, R. Blankenbecler, *Phys. Rev.* **128**, 415 (1962).
- [16] P. Giromini, Proc. of Vth Blois Workshop — International Conference on Elastic and Diffractive Scattering, Providence, RI, 8-12 Jun 1993, Editors H.M. Fried, K. Kang and C-I Tan, World Scientific (Singapore), 1994 p. 30.
- [17] P.M. Nadolsky, S.M. Troshin, N.E. Tyurin, Z. Phys. C **69**, 131 (1995).
- [18] S. M. Troshin and N. E. Tyurin, Teor. Mat. Fiz. **28**, 139 (1976) .
- [19] S.M. Troshin, N.E. Tyurin, Z. Phys. C **45**, 171 (1989).
- [20] N. Sakai, Nuovo Cimento A **21**, 368 (1974).
- [21] J.D. Bjorken, Nucl. Phys. Proc. Supl. **25B**253 (1992).
- [22] D. Diakonov, Eur. Phys. J. A **24s1**, 3 (2005).
- [23] T. Goldman, R.W. Haymaker, Phys. Rev. D **24**, 724 (1981).

- [24] W. Heisenberg, Z. Phys. **133**, 65 (1952).
- [25] P. Carruthers, Nucl. Phys. A **418**, 501 (1984).
- [26] D. Diakonov, V. Petrov, Phys. Lett. B **147**, 351 (1984).
- [27] K. Adcox, et al., Nucl. Phys. A **757**, 184 (2005).
- [28] J. Castillo (for the STAR Collaboration), Int. J. Mod. Phys. A20 (2005) 4380.
- [29] S. M. Troshin, N. E. Tyurin, Phys. Rev. D **49**, 4427 (1994).
- [30] J. Zimányi, P. Lévai, T.S. Biró, hep-ph/0205192.
- [31] S.M. Troshin, N.E. Tyurin, Int. J. Mod. Phys. E **17**, 1619 (2008).
- [32] Quark Gluon Plasma. New Discoveries at RHIC: A Case of Strongly Interacting Quark Gluon Plasma. Proceedings, RBRC Workshop, Brookhaven, Upton, USA, May 14-15, 2004: D. Rischke, G. Levin, eds; 2005, 169pp.
- [33] R. Hagedorn, Nuovo Cim. Suppl. **3**, 147 (1965).
- [34] The CMS Collaboration, arXiv: 1002.0621v1 [hep-ex].
- [35] T.S. Ullrich, Nucl. Phys. A **715**, 399 (2003).
- [36] T.T. Chou, C.-N. Yang, Int. J. Mod. Phys. A **6**, 1727 (1987).
- [37] S.M. Troshin, N.E. Tyurin, Mod. Phys. Lett. A **25**, 1315 (2010).
- [38] D. Molnar, S.A. Voloshin, Phys. Rev. Lett. **91**, 092301 (2003).
- [39] S.A. Voloshin, Acta Physica Polonica B **36**, 551 (2005) .
- [40] STAR Collaboration, B. I. Abelev et al. , Phys. Rev. Lett. **105**, 022301 (2010).
- [41] CMS Collaboration, V. Khachatryan et al., JHEP **1009**, 091 (2010).
- [42] E. Shuryak, arXiv:1009.4635[hep-ph].
- [43] A. Dumitru *et al.*, Phys. Lett. B 697 (2011) 21; arXiv:1009.5295[hep-ph].
- [44] P. Bozek, Eur. Phys. J. C 71 (2011) 1530; arXiv:1010.0405 [hep-ph].
- [45] I.M. Dremin, V.T. Kim, Pisma ZhETF 92 (2011) 720; arXiv:1010.0918[hep-ph].
- [46] T.A. Trainor, D.T. Kettler, arXiv:1010.3048[hep-ph].
- [47] I.O. Cherednikov, N.G. Stefanis, arXiv:1010.4463[hep-ph].
- [48] A. Kovner and M. Lublinsky, Phys. Rev. D **83**, 034017 (2011).

- [49] K. Werner, Iu. Karpenko, T. Pierog, Phys. Rev. Lett. **106**, 122004 (2011).
- [50] M.Yu. Azarkin, I.M. Dremin, A.V. Leonidov, arXiv:1102.3258[hep-ph].
- [51] R. C. Hwa and C. B. Yang, Phys. Rev. C **83**, 024911 (2011).
- [52] B.A. Arbuzov, E.E. Boos, V.I. Savrin, arXiv: 1011.1283 [hep-ph].
- [53] S.M. Troshin, N.E. Tyurin, arXiv: arXiv:1009.5229 [hep-ph].
- [54] D. Miskowiec, arXiv:0707.0923 [hep-ph].
- [55] Xu Mingmei, Yu Meiling, Liu Lianshou, Phys. Rev. Lett. **100**, 092301 (2008).
- [56] L.L. Jenkovszky, A. Nagy, S.M. Troshin, J. Turoci, N.E. Tyurin, Int. J. Mod. Phys. A **25**, 5667 (2010) .
- [57] B.R. Webber, Nucl. Phys. B **87**, 269 (1975).
- [58] J. Benecke, T.T. Chou, C.N. Yang, E. Yen, Phys. Rev. **188**, 2159 (1969).
- [59] M.M. Islam, R.J. Luddy, A.V. Prokudin, Mod. Phys. Lett. A **18**, 743 (2003).